

DOI: 10.1002/cbic.201000055

Unusual η^2 -Allene Osmacycle with Apoptotic Properties

Xumin He,^[a] Lei Gong,^[a] Katja Kräling,^[b] Katharina Gründler,^[c] Corazon Frias,^[c] Richard D. Webster,^[d] Eric Meggers,^{*[b]} Aram Prokop,^{*[c]} and Haiping Xia^{*[a]}

Screening of a library of structurally unusual osmacyclic complexes for their antiproliferate properties in HeLa cells led to the discovery of a highly cytotoxic η^2 -allene osmacycle. In this remarkably stable complex, osmium constitutes part of a metallacycle through the formation of a σ -bond to a carbon in combination with coordination to an allene moiety. The osmacycle strongly induces apoptosis in Burkitt-like lymphoma cells at submicromolar concentrations. The reduction of the mito-

chondrial membrane potential, the induction of DNA fragmentation, and the activation of caspases-9 and -3 reveal that programmed cell death occurs through the intrinsic mitochondrial pathway. From the lipophilic and cationic nature of the osmacycle, in addition to a low oxidation potential ($E_{1/2} = +0.27$ V vs. Fc/Fc⁺, Fc = ferrocene) it is proposed that mitochondria are the cellular target where oxidative decomposition initiates apoptosis.

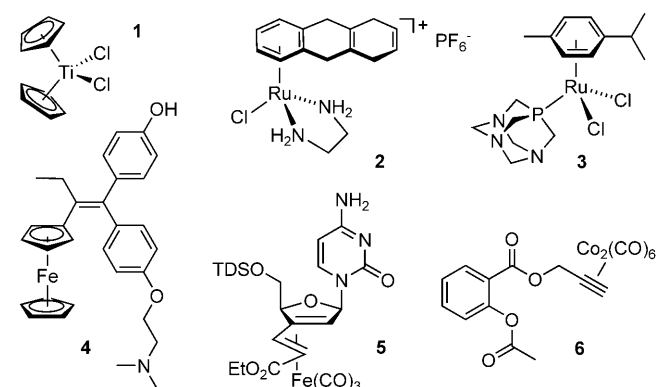
Introduction

Organometallic molecular scaffolds often display unconventional structures and/or reactivities, making them an attractive, underexplored source in the search for novel anticancer agents.^[1] In 1979, only about a decade after the seminal discovery of cisplatin, the most successful metal-containing anticancer drug, Köpf and Köpf-Maier revealed the promising anticancer activity of titanocene dichloride (**1**, Scheme 1).^[2] Al-

between the ruthenium complexes and the guanine bases of genomic DNA.^[5] In contrast, the ruthenium(II)-arene-pta complexes (pta = 1,3,5-triaza-7-phosphaadamantane) developed by Dyson and co-workers display low cytotoxicities in vitro but remarkable effects on metastasis in vivo.^[6]

Our group followed a different strategy by designing a class of unreactive ruthenium and osmium η^5 -cyclopentadienyl pyridocarbazole complexes that bind reversibly to the ATP-binding sites of protein kinases, with some complexes displaying strong apoptotic properties in vitro.^[8] In a related approach, Keppler and co-workers modified the protein kinase inhibitor paullone with ruthenium(II)-arene half-sandwich fragments, making the resulting complexes highly active in vitro.^[9]

Jaouen and co-workers pioneered a class of ferrocene-based anticancer drug candidates.^[10] Replacement of, for example, a phenyl moiety of tamoxifen, an antagonist of the estrogen receptor and clinical drug for hormone-positive breast cancer,



Scheme 1. Selection of organometallic complexes reported to display anticancer activities. TDS = thexyldimethylsilyl.

though clinical trials of this early organometallic anticancer drug candidate were eventually abandoned, improvement of this scaffold by derivatization is still an active area of research.^[3,4]

More recently, a series of ruthenium(II)- and osmium(II)-arene half-sandwich complexes have emerged as new anticancer agents.^[5–7] Sadler and co-workers, for example, developed $[\eta^6\text{-arene}]\text{Ru}(\text{en})\text{Cl}]^+$ complexes (e.g., complex **2** in Scheme 1 with arene = tetrahydroanthracene) that exhibit high cytotoxicities against a variety of cancer cell lines and in tumours grafted on mice, most likely induced through reactions

[a] Prof. Dr. X. He, Dr. L. Gong, Prof. Dr. H. Xia
State Key Laboratory of Physical Chemistry of Solid Surfaces
College of Chemistry and Chemical Engineering, Xiamen University
Xiamen, 361005 (China)
Fax: (+86) 592-218-6628
E-mail: hpxia@xmu.edu.cn

[b] K. Kräling, Prof. Dr. E. Meggers
Fachbereich Chemie, Philipps-Universität Marburg
Hans-Meerwein-Strasse, 35032 Marburg (Germany)
Fax(+49) 6421-2821535
E-mail: meggers@chemie.uni-marburg.de

[c] K. Gründler, C. Frias, Dr. A. Prokop
Kliniken der Stadt Köln gGmbH
Neufelder Strasse 34, 51067 Köln (Germany)
Fax: (+49) 221-89075395
E-mail: prokopa@kliniken-koeln.de

[d] Prof. Dr. R. D. Webster
Division of Chemistry and Biological Chemistry
School of Physical and Mathematical Sciences
Nanyang Technological University
SPMS-CBC-04-06, 21 Nanyang Link, Singapore 637371 (Singapore)

provided the so-called class of organometallic ferrocifens **3** (Scheme 1), which exhibit strong antiproliferate properties in hormone-independent breast cancer cells. Most likely, the redox properties of the ferrocene are a key feature of the mode of action of this class of anticancer complexes.

It is striking that most thoroughly investigated organometallic anticancer scaffolds contain half-sandwich or sandwich moieties, although exceptions include the apoptotic iron nucleoside complex **5** discovered by Schmalz and co-workers and the antitumour-active cobalt-alkyne complex **6** developed by Gust, Ott, and co-workers.^[11,12] However, it is likely that neglected, unusual organometallic scaffolds provide untapped opportunities to be exploited for the discovery and development of compounds with surprising and novel biological properties.

We wish to report here the highly apoptotic properties of an unusual organometallic η^2 -allene osmacycle. Despite its chemical stability, the complex strongly induces apoptosis in Burkitt-like lymphoma cells and we demonstrate that this occurs through the intrinsic mitochondrial pathway of programmed cell death.

Results and Discussion

Screening of an osmacycle library for anticancer activities

Osmium has the ability to form remarkably diverse, yet stable organometallic complexes with unusual bonds to carbon. Here we focused on the class of osmacyclic^[13] organometallics and assembled a selection of osmium complexes **OC1–10** (Scheme 2), including three osmabenzenes (**OC1–3**),^[14,15] two osmafurans (**OC4, OC5**),^[16] a bicyclic osmium complex (**OC5**),^[16] an allenolate osmacycle (**OC6**),^[16] a cyclic osmatriene complex (**OC7**),^[17] a cyclometalated pentadienone complex (**OC8**),^[18] a nine-membered osmacycle (**OC9**),^[16] and a metallacyclic eneallene complex (**OC10**). A screening of this small library of osmacyclic complexes for cytotoxic properties in HeLa cancer cells revealed large differences in the efficacies of individual library members, over a range of almost two orders of magnitude. Whereas the osmabenzenes **OC1–3** displayed very modest cytotoxicities, with EC_{50} values (compound concentrations at

which the viabilities of HeLa cells are reduced to 50% after 24 h incubation) in the range of 10 μM for **OC1** to greater than 30 μM for **OC3** (83% cell survival at 30 μM and 24 h), the osmafuran complex **OC4** showed a significant anticancer effect with $EC_{50} = 4 \mu\text{M}$. In contrast, the osmafuran complex **OC5** was too hydrophobic to be dissolvable in DMSO and could therefore not be tested. The allenolate osmacycle **OC6** exerted only a weak effect on HeLa cells ($EC_{50} = 20 \mu\text{M}$), whereas the osmacycles **OC7–10** displayed cytotoxicities in the lower micromolar range, with the complexes **OC9** and **OC10** being most potent with EC_{50} values of about 1 μM each. Figure 1 shows a concentration-dependent cytotoxicity profile of **OC10** in HeLa cells, demonstrating virtually complete extinction of HeLa cells at a concentration of 10 μM **OC10** after incubation for 24 h. Because of its high potency in combination with its unique structure and remarkably high stability (see below), we selected the η^2 -allene osmacycle **OC10** for further studies.

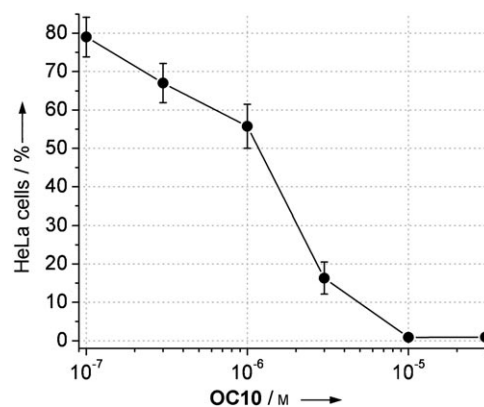
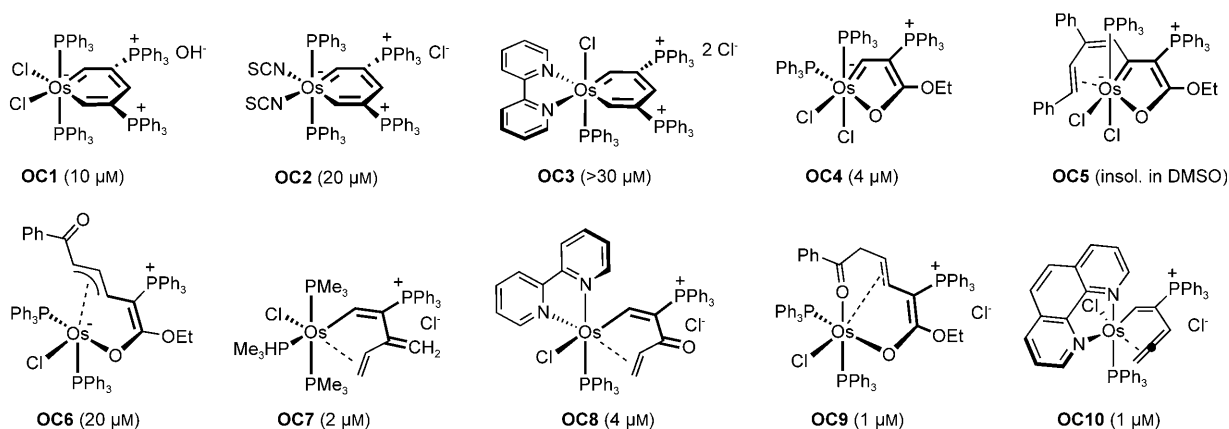


Figure 1. Cytotoxicity of osmacycle **OC10** in HeLa cells. Cells were incubated with **OC10** at different concentrations for 24 h and cell survival was determined by the MTT method.

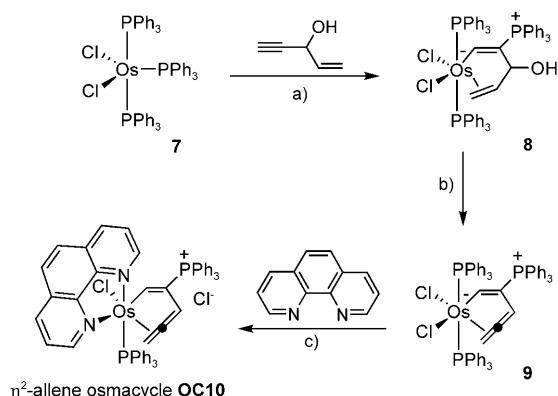
Synthesis and structure of the η^2 -allene osmacycle **OC10**

The osmacycle **OC10** was synthesised in three steps from the readily accessible $[\text{Os}(\text{PPh}_3)_3\text{Cl}_2]$ (**7**)^[19] in an overall yield of 43%



Scheme 2. Screening of a diverse selection of unusual osmacycles **OC1–10** for their antiproliferate properties in HeLa cells. Shown in brackets are half-maximum effective concentrations (EC_{50} values) at which the viabilities of HeLa cells are reduced to 50% after 24 h incubation at the given concentrations.

(Scheme 3). Treatment of **7** with $\text{HC}\equiv\text{CCH}(\text{OH})\text{CH}=\text{CH}_2$ in THF at 0°C for 1 h afforded the η^2 -allyl osmacycle **8** (65%), which was followed by conversion into the allene complex **9** in the



Scheme 3. Synthesis of the osmacycle **OC10**. a) THF, 0°C , 65%; b) AcOH, CH_2Cl_2 , reflux, 76%; c) CH_2Cl_2 , 88%.

presence of acetic acid in CH_2Cl_2 under reflux (76%).^[20] Finally, the substitution of one phosphine and one chloride by 1,10-phenanthroline in CH_2Cl_2 at room temperature provided the osmacycle **OC10** in 88% yield.

A crystal structure of the monocation of **OC10** is shown in Figure 2. The unusual structure contains a conjugated osmacycle with an allene coordinated to the osmium in a η^2 -fashion through the terminal double bond. The osmacycle can be viewed as a five-membered ring, consisting of Os1 and C1–C4, with an additional exocyclic methylene group C5 coordinated to the osmium centre. The terminal coordinated C4=C5 double

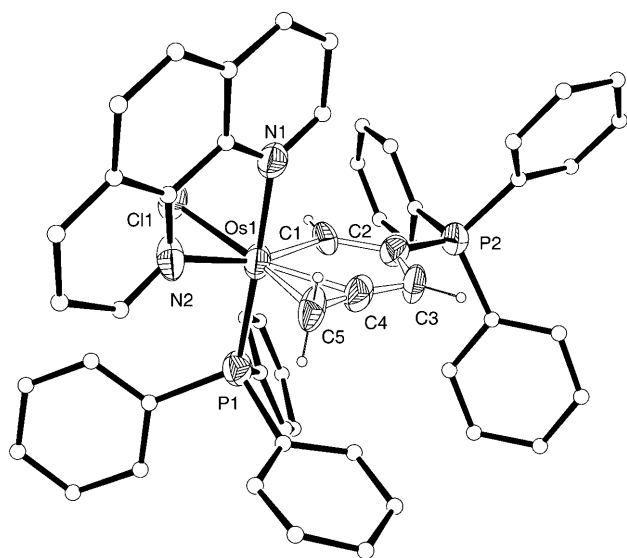


Figure 2. Crystal structure of the complex cation of **OC10** at the 50% probability level. Selected interatomic distances [Å] and angles [°]: Os1–C1 = 2.033(8), Os1–C4 = 2.061(9), Os1–C5 = 2.156(10), C1–C2 = 1.369(13), C2–C3 = 1.448(15), C3–C4 = 1.283(15), C4–C5 = 1.419(15); C1–Os1–C4 = 72.6(4), C2–C1–Os1 = 120.1(8), C1–C2–C3 = 112.6(9), C2–C3–C4 = 110.5(9), C3–C4–C5 = 161.5(10), C5–C4–Os1 = 66.8(5).

bond is almost in plane with the osmacycle. The osmium is additionally coordinated in a distorted octahedral geometry by PPh_3 , by chloride and by 1,10-phenanthroline.

The osmacycle **OC10** has excellent thermostability and air-stability as a solid, remaining nearly unchanged at 200°C for 5 h under air. Moreover, the chemical stability of **OC10** in solution is also remarkable for such an unconventional structure. Unlike **9** or related coordinated allene complexes, the osmacycle **OC10** undergoes neither ligand substitutions nor nucleophilic or electrophilic additions to the terminal allene. For example, **OC10** remained unchanged when treated with CO, PMe_3 , DMSO, 1,10-phenanthroline, NaI, NaSCN, or CH_3I for several days at room temperature. Furthermore, **OC10** can also withstand high concentrations of thiols (DMSO/ H_2O / β -mercaptoethanol 5:1:1) and a buffered amine solution for several hours. It can thus be expected that the osmacycle **OC10**, despite its unusual structure, should stay intact in a biological cell harbouring millimolar concentrations of nucleophilic thiols and amines.^[21]

Anticancer activity of **OC10** in Burkitt-like lymphoma cells

We next tested the anticancer properties of osmacycle **OC10** in Burkitt-like lymphoma (BJAB) which is clinically classified as an aggressive cancer with unfavourable survival statistics. Interestingly, the treatment of BJAB cells with **OC10** for 24 h already resulted in inhibition of proliferation at concentrations below $1\ \mu\text{M}$, as shown in Figure 3, whereas no induction of ne-

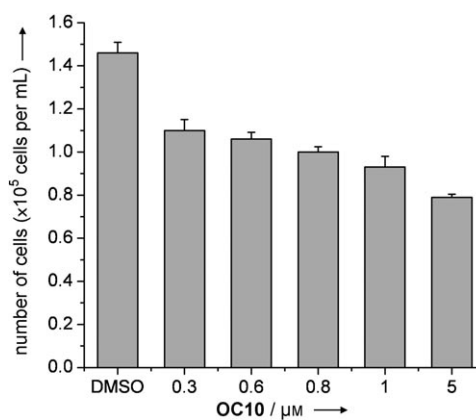


Figure 3. Antiproliferate effect of **OC10** in BJAB cells. Inhibition of cell proliferation after treatment with **OC10** for 24 h as measured by a CASY cell counter. Bars indicate the number of cells after 24 h incubation. DMSO-treated cells served as the control.

rosis could be detected at these concentrations as determined with a lactate dehydrogenase release assay.^[22] To gain more insight into the reasons for the osmacycle-induced antiproliferate effect in BJAB cells, a flow cytometric cell cycle analysis was performed after incubation of BJAB cells with **OC10** for 72 h. The results are shown in Figure 4 and reveal a dose-dependent induction of apoptosis in BJAB cells after treatment with **OC10**. Compound **OC10** potently induced DNA fragmentation in 25% of the cells even at $0.3\ \mu\text{M}$ and in up to 75% of

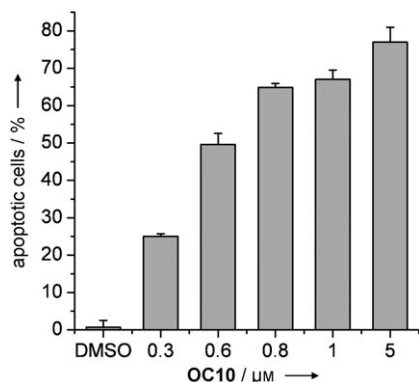


Figure 4. Apoptotic properties of **OC10** in BJAB cells. Induction of apoptosis measured by DNA fragmentation after treatment of BJAB cells with **OC10** for 72 h. Nuclear DNA fragmentation was quantified by flow cytometric determination of hypodiploid DNA. Data are given in percentage hypodiploidy (sub-G1) \pm SD ($n=3$), which reflects the number of apoptotic cells.

the cells at a concentration of 5 μM . These data verify highly efficient induction of apoptosis by **OC10**.

The induction of programmed cell death is an important mode of action of anticancer drugs.^[23] The intrinsic pathway of cell death proceeds following mitochondrial outer membrane permeabilization, release of cytochrome c, caspase-9 activation and ultimately the activation of the executioner caspases-3, -6 and -7. To determine the involvement of mitochondrial-mediated apoptosis, mitochondrial activation was measured after treatment of BJAB cells with **OC10** for 48 h. Exposure to **OC10** resulted in a strong reduction in the mitochondrial membrane potential as determined by staining with the dye JC-1. At an **OC10** concentration of 0.6 μM , for example, over 40% of BJAB cells displayed reduced membrane potentials after 48 h (Figure 5A). Additionally, caspase-9 and -3 activation were investigated for more specific confirmation of the intrinsic pathway. As illustrated in Figure 5B, procaspase-9 degradation was analysed by Western blot analysis after incubation of the BJAB cells with the osmacycle **OC10** (1 μM and 5 μM), revealing a significant level of processed caspase-9 levels induced by **OC10**. At the same time the procaspase-3 levels decreased as a function of increasing concentrations of **OC10**. Our investigations thus reveal that the osmacycle **OC10** triggers the mitochondrial pathway of apoptosis.

Anticancer activity in drug-resistant leukaemia cells

Multidrug resistance is a phenomenon of simultaneous resistance to unrelated chemotherapeutic drugs often caused by active transport of toxic compounds out of the cell, thus constituting an immediate obstacle for the therapeutic treatment of tumours.^[24] Anthracyclines such as daunorubicin (Dau) and vinca alkaloids such as vincristine (Vcr) are potent agents used in cytotoxic chemotherapy, and the occurrence of resistance against Vcr and Dau and other drugs is a serious problem in clinical oncology.^[25] We were therefore interested in testing the effect of **OC10** on Vcr- and Dau-resistant cancer cell lines. Accordingly, regular leukaemia cells (Nalm6), Vcr-resistant Nalm6

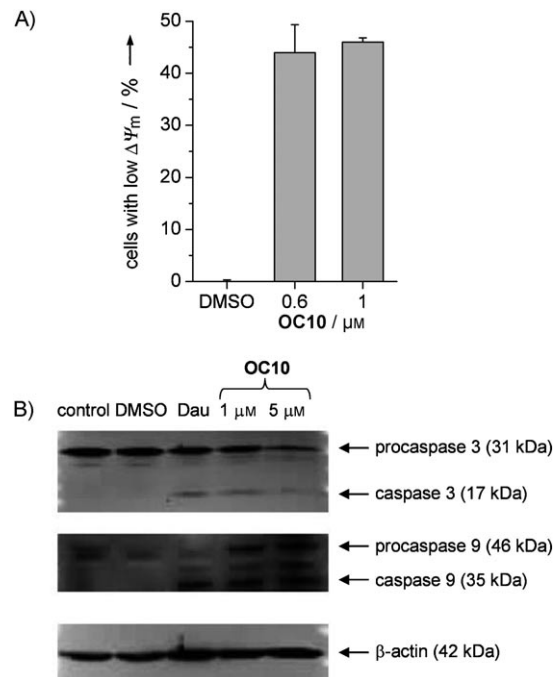


Figure 5. Probing the induction of apoptosis by **OC10** by the intrinsic pathway. A) Influence of **OC10** on the membrane potential ($\Delta\Psi_m$): The mitochondrial permeability transition was measured by flow cytometric analysis in BJAB cells after treatment with various concentrations of **OC10** for 48 h. Values of the mitochondrial permeability transition are given as the fraction of cells with decreased membrane potential in $\% \pm$ SD ($n=3$). B) Procaspase-9 and -3 degradation: BJAB cells were incubated for 48 h with daunorubicin (Dau, 60 nM; lane 3, positive control), **OC10** (1 μM , lane 4) and **OC10** (5 μM , lane 5). Lane 1 shows untreated cells and lane 2 DMSO-treated cells. Cytosolic proteins (20 μg) were separated by SDS-PAGE, subjected to Western blot analysis, and immunoblotted with anticaspase-9 and anticaspase-3 antibodies. Equal loading and blotting was verified by detection of the 42 kDa β -actin.

cells and Dau-resistant Nalm6 cells were treated with **OC10** for 72 h and apoptosis induction was determined by flow cytometry measurements. Figure 6A depicts the apoptosis induction in Vcr-resistant leukaemia cells, whereas the apoptosis induction in Dau-resistant leukaemia cells is displayed in Figure 6B. These in vitro experiments with the human B-cell precursor leukaemia cell line Nalm6 reveal that **OC10** cannot overcome drug resistance in vincristine-resistant and daunorubicin-resistant cells at lower concentrations (1 μM), but is effective at higher concentrations (5 μM).

Cyclic voltammetry

Lipophilic cations, such as triphenylphosphonium cations, accumulate in the mitochondria as a result of the large mitochondrial membrane potential.^[26,27] Because of the elevated mitochondrial membrane potentials of many tumour tissues, this mode of action is promising for the development of mitochondria-targeting anticancer agents that are selective for cancer cells.^[26,27] It can be speculated that the cationic osmacycle targets the mitochondria as a result of its high hydrophobicity, resulting from the presence of a coordinated triphenylphosphine ligand in combination with a triphenylphosphoni-

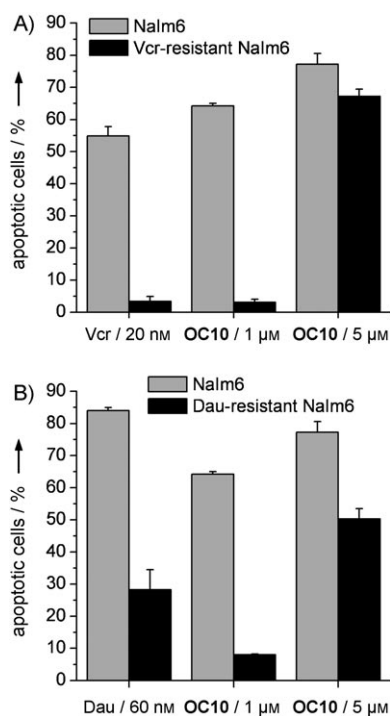


Figure 6. Apoptosis induced by the osmacycle **OC10** in vincristine-resistant (Vcr-resistant) and daunorubicin-resistant (Dau-resistant) leukaemia cells. Apoptosis was determined by DNA fragmentation in regular leukaemia cells (Nalm6), and A) Vcr-resistant Nalm6 cells, and B) Dau-resistant Nalm6 cells after an incubation period of 72 h with various concentrations of the indicated drugs. Data are given in percentage hypodiploidy (sub-G1) \pm SD ($n=3$), which reflects the number of apoptotic cells.

um moiety. Once inside the mitochondria, oxidative processes might trigger the conversion of the cation of **OC10** into a reactive species that could initiate programmed cell death. In order to probe this hypothesis, we conducted cyclic voltammetry (CV) experiments with **OC10** in MeCN and CH_2Cl_2 (Figure 7). The voltammograms reveal that **OC10** can be reduced in an irreversible multielectron process at high negative potential and reversibly oxidized in a one-electron process. Interestingly, the oxidation potential is quite low, at +0.27 V versus ferrocene/ferrocenium ion in MeCN, thus supporting the hypothesis that **OC10** might be prone to oxidation once inside the mitochondria.

Conclusions

In conclusion, here we report the promising anticancer activity of the novel osmacyclic compound **OC10** for the first time. Despite its chemical stability, **OC10** strongly induces apoptosis in Burkitt-like lymphoma cells at submicromolar concentrations and we have demonstrated that this occurs through the intrinsic mitochondrial pathway of programmed cell death. The results presented here thus indicate that unusual, previously unconsidered organometallics provide untapped opportunities to be exploited for the discovery and development of future drug candidates.

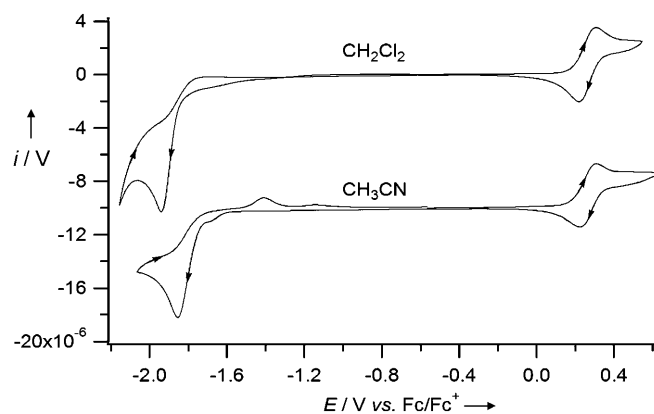


Figure 7. Cyclic voltammograms of the osmacycle **OC10** (with PF_6^- as counter ion, 2 mM, 5 mL of solvent) recorded at a scan rate of 0.1 V s^{-1} in deoxygenated CH_2Cl_2 and CH_3CN containing Bu_4NPF_6 (0.2 M) at a 1 mm diameter Pt electrode at $22 \pm 2^\circ\text{C}$. Fc = ferrocene. Oxidation process: $E_{1/2} = +0.264 \text{ V}$ (CH_2Cl_2), $+0.266 \text{ V}$ (CH_3CN).

Experimental Section

Synthesis of osmacycles: The complexes **OC1–OC9** have been reported recently.^[14–18] The osmacycle **OC10** was synthesised as follows. A mixture of 1,10-phenanthroline monohydrate (118.8 mg, 0.60 mmol) and the osmacycle **9**^[20] (0.33 g, 0.30 mmol) in CH_2Cl_2 (dried over CaH_2 , 15 mL) was stirred under nitrogen at room temperature for about 5 h to give a red solution. The volume of the mixture was reduced under vacuum to approximately 2 mL. Addition of diethyl ether (15 mL) to the solution gave a red precipitate, which was collected by filtration, washed with THF (5 \times 2 mL) and then dried under vacuum. Yield: 0.27 g, 88%. ^1H NMR (300.1 MHz, CDCl_3): $\delta = 11.9$ (d, $^3J(\text{P,H}) = 18.0 \text{ Hz}$, 1H, OsCH), 7.4 (d, $^3J(\text{P,H}) = 6.8 \text{ Hz}$, 1H, OsCHC(PPh₃)CH, obscured by the phenyl signals and confirmed by $^1\text{H}, ^{13}\text{C}$ COSY), 3.0 (dd, $^2J(\text{H,H}) = 6.9 \text{ Hz}$, $^3J(\text{P,H}) = 6.0 \text{ Hz}$, 1H, CCH₂), 2.2 (d, $^2J(\text{H,H}) = 6.9 \text{ Hz}$, 1H, CCH₂), 7.2–9.3 ppm (m, 38H, PPh₃ and 1,10-phen); $^{13}\text{C}\{^1\text{H}\}$ NMR (75.5 MHz, CDCl_3): $\delta = 209.1$ (d, $^3J(\text{P,C}) = 7.5 \text{ Hz}$, OsCH), 193.9 (d, $^3J(\text{P,C}) = 23.4 \text{ Hz}$, CHCCH₂), 119.4 ppm (d, $^1J(\text{P,C}) = 74.0 \text{ Hz}$, C(PPh₃)); $^{31}\text{P}\{^1\text{H}\}$ NMR (121.5 MHz, CDCl_3): $\delta = 9.1$ (d, $^3J(\text{P,P}) = 3.6 \text{ Hz}$, C(PPh₃)), -5.6 (d, $^3J(\text{P,P}) = 3.6 \text{ Hz}$, OsPPh₃), 117.8 (d, $^2J(\text{P,C}) = 26.4 \text{ Hz}$, CHCCH₂), 26.5 (s, CCH₂), 121.9–154.3 ppm (m, PPh₃ and 1,10-phen); elemental analysis calcd (%) for $\text{C}_{53}\text{H}_{42}\text{N}_2\text{P}_2\text{Cl}_2\text{Os}$: N 2.72, C 61.80, H 4.11; found: N 2.82, C 61.43, H 4.27.

Evaluation of OC10 stability

Stability against some nucleophiles and the electrophile CH_3I : PMe_3 , 1,10-phenanthroline, NaI, NaSCN, DMSO or CH_3I (0.10 mmol) was added under nitrogen to a solution of **OC10** (10.3 mg, 0.010 mmol) in CDCl_3 (0.5 mL) in an NMR tube and the solution was mixed with the aid of ultrasound. The ^1H NMR spectra remained unchanged after three days at room temperature. **OC10** remained stable under an atmosphere of CO under the same conditions.

Stability against thiols: Compound **OC10** (about 5 mg, about 5 μmol) was incubated at room temperature in $[\text{D}_6]\text{DMSO}/\text{D}_2\text{O}$ (5:1, 0.6 mL) in the presence of β -mercaptoethanol (0.1 mL, 1.4 mmol). No signs of decomposition could be detected after 7 h as determined by ^1H NMR analysis.

Stability against amines: Compound **OC10** (5.2 mg, 5 μmol) in DMSO (0.5 mL) was added to a solution of methylamine (4.4 μL , 50 μmol , 40% aqueous solution) in sodium phosphate buffer

(2 mL, 100 mM, pH 7.0). The mixture was stirred at room temperature. After 1 h, a portion of the sample was concentrated under vacuum, the remaining residue was extracted three times with CH_2Cl_2 , and the combined organic phase was evaporated under vacuum, washed with diethyl ether and finally dried under high vacuum. ^1H and ^{31}P NMR spectra demonstrated that the starting material remained unchanged. Another portion of the sample was worked up in the same fashion after 24 h and showed that 85% of the compound remained intact.

Crystal structure of OC10: Single crystals of OC10 suitable for X-ray diffraction were grown from CH_2Cl_2 solutions layered with ether. A selected crystal was mounted on top of a glass fibre and transferred into a cold stream of nitrogen. Data collections were performed with an Oxford Gemini S Ultra CCD Area Detector and use of graphite-monochromated $\text{MoK}\alpha$ radiation ($\lambda = 0.71073 \text{ \AA}$). Empirical absorption corrections were carried out with SADABS. The structure was solved by direct methods, expanded by difference Fourier synthesis, and refined by full-matrix, least-squares on F^2 with the aid of the Bruker SHELXTL-97 program package. Non-hydrogen atoms were refined anisotropically. Hydrogen atoms were introduced at their geometric positions and refined as riding atoms. Crystallographic data: $\text{ClO}_5\text{P}_2\text{N}_2\text{C}_{53}\text{H}_{42} \cdot 0.5 \text{CH}_2\text{Cl}_2 \cdot 2\text{H}_2\text{O}$, $M = 1073.0$, monoclinic, $a = 15.288(2)$, $b = 10.417(1)$, $c = 32.130(4) \text{ \AA}$, $\alpha = 90^\circ$, $\beta = 100.369(2)^\circ$, $\gamma = 90^\circ$, $V = 5033.6(12) \text{ \AA}^3$, $\text{Mo } \alpha$ ($\lambda = 0.71073 \text{ \AA}$) radiation at $223(2) \text{ K}$, space group $P21/n$, $Z = 4$, 35 695 reflections measured, 8865 unique ($R_{\text{int}} = 0.0844$) which were used in all calculations. R_1 [$I > 2\sigma(I)$] = 0.0799, wR_2 (all data) = 0.2439.

CCDC 675410 contains the supplementary crystallographic data for this paper. These data can be obtained free of charge from The Cambridge Crystallographic Data Centre via www.ccdc.cam.ac.uk/data_request/cif.

Cytotoxicity measurements with Hela cells: Hela cells were maintained in Dulbecco's modified Eagle's medium (DMEM) supplemented with fetal bovine serum (FBS; 10%), glutamate (1%) and penicillin/streptomycin (1%) at 37°C under CO_2 (5%) and constant humidity. Cells were plated into 96-well plates (9000–10000 cells per well) and left to attach for 24 h. Afterwards, different concentrations of osmacycles as stock solutions in DMSO were added (resulting in final concentrations of 1% DMSO) and cells were incubated with the compounds for 24 h. As a control, the same number of cells was treated with DMSO (1%). After the incubation period, the medium was replaced with fresh medium (200 μL) and 3-(4,5-dimethylthiazol-2-yl)-2,5-diphenyltetrazolium bromide (MTT, 5 mg mL^{-1} , 20 μL). Cells were incubated with MTT for 3 h and after that time the medium (155 μL) was removed and DMSO (90 μL) was added to solubilize the resulting purple crystals. After 10 min, the absorbance of each well was measured at 535 nm. Cell survival at different inhibitor concentrations was calculated as a percentage of the control absorbance (subtraction of the background absorption of culture media with MTT and 1% DMSO). Each experiment was repeated in quadruplet.

Cell culture with BJAB and Nalm6 cells: BJAB and Nalm6 cells were cultured at 37°C in RPMI 1640 (GIBCO, Invitrogen) supplemented with heat-inactivated (FBS; 10%), penicillin (10^5 U L^{-1}), streptomycin (0.1 g L^{-1}) and L-glutamine (0.56 g L^{-1}). The cells were subcultured every 3–4 days by diluting the cells to a concentration of $1 \times 10^5 \text{ cells mL}^{-1}$. To ascertain standardized growth conditions, cells were cultured 24 h before the assay setup to a concentration of $3 \times 10^5 \text{ cells mL}^{-1}$. For the experiments cells were diluted to a concentration of $1 \times 10^5 \text{ cells mL}^{-1}$ immediately before addition of the osmacycle OC10.

Determination of cell viability in BJAB and Nalm6 cells: Cell viability was determined by CASY® (Cell counter and Analyzer System, Innovatis, Bielefeld, Germany). Settings were specifically defined for the requirements of the cells used. The cell concentrations were analysed simultaneously in three different size ranges: cell debris, dead cells, and viable cells. After a 24 h incubation period at 37°C , cells were resuspended properly, and 100 μL of each well was diluted in CASYton (ready-to-use isotonic saline solution, 10 mL) for immediate automated counting of the cells.

Lactate dehydrogenase release assay:^[22] BJAB cells were incubated with various concentrations of OC10 for 1 h at 37°C , and the activity of lactate dehydrogenase (LDH), early release of which is characteristic for necrotic cell death, was measured in the cell culture supernatants with the cytotoxicity detection kit from Boehringer Mannheim. The supernatants were centrifuged at 1500 rpm for 5 min and cell-free supernatants (20 μL) were then diluted with phosphate-buffered saline (PBS, 80 μL) and reaction mixture (100 μL). Time-dependent formation of the reaction product was quantified photometrically at 490 nm. The maximum amount of LDH activity released by the cells was determined by lysis of the cells by use of Triton X-100 in culture medium (0.1%) and set as 100%. Under these conditions, less than 5% LDH release was observed up to an OC10 concentration of 10 μM .

Measurement of DNA fragmentation in BJAB cells: Apoptotic cell death was determined by a modified cell-cycle analysis that detects DNA fragmentation at the single-cell level as described previously.^[28,29] After a 72 h incubation period at 37°C , cells were collected by centrifugation at 1500 rpm for 5 min, washed with PBS at 4°C and fixed in PBS/formaldehyde (2%, v/v) on ice for 30 min. After fixation, cells were incubated with EtOH/PBS (2:1, v/v) for 15 min, pelleted and resuspended in PBS containing RNase A ($40 \mu\text{g mL}^{-1}$). RNA was digested for 30 min at 37°C , after which the cells were pelleted once again and finally resuspended in PBS containing propidium iodide ($50 \mu\text{g mL}^{-1}$). Nuclear DNA fragmentation was quantified by flow cytometric determination of hypodiploid DNA (fluorescence-activated cell sorting, FACS). Data were collected and analysed by use of a FACScan (Becton Dickinson, Heidelberg, Germany) apparatus with CELL Quest software. Data are given in % hypodiploidy (sub-G₁).

Measurement of the mitochondrial permeability transition in BJAB cells: After an incubation period of 48 h with various concentrations of the OC10 complex, cells were collected by centrifugation at 1500 rpm at 4°C for 5 min. The mitochondrial permeability transition was then determined by staining the cells with 5,5',6,6'-tetrachloro-1,1',3,3'-tetraethylbenzimidazolylcarbocyanine iodide (JC-1, Molecular Probes). Cells were resuspended in phenol-red-free RPMI 1640 without supplements (500 μL), and JC-1 was added to a final concentration of $2.5 \mu\text{g mL}^{-1}$. The cells were incubated for 30 min at 37°C with moderate shaking. Control cells were likewise incubated in the absence of JC-1 dye. The cells were harvested by centrifugation at 1500 rpm and 4°C for 5 min, washed with ice-cold PBS and resuspended in PBS (200 μL) at 4°C . Mitochondrial permeability transition was then quantified by flow cytometric determination of the cells with decreased fluorescence (that is, with mitochondria displaying lower membrane potentials). Data were collected and analysed by use of a FACScan (Becton Dickinson, Heidelberg, Germany) apparatus and CELL Quest software. Data are given as percentages of the cells with low mitochondrial membrane potential.

Immunoblotting: After incubation for 48 h with different concentrations of OC10, BJAB cells were washed twice with PBS and lysed

in buffer containing Tris/HCl (10 mM, pH 7.5), NaCl (300 mM), Triton X-100 (1%), MgCl₂ (2 mM), EDTA (5 μM), pepstatin (1 μM), leupeptin (1 μM) and phenylmethylsulfonyl fluoride (PMSF, 0.1 mM). Protein concentration was determined by Pierce's bicinchoninic acid assay, and equal amounts of protein were separated by SDS-PAGE.^[30] Immunoblotting was performed at 1 mA cm⁻² for 1 h in a Transblot SD cell (BioRad, München, Germany). The membrane was blocked for 1 h in PBST (PBS, 0.05% Tween-20) containing 5% non-fat dry milk and incubated with primary anti-mouse caspase-3 antibody (Santa Cruz Biotechnology Inc., Santa Cruz, USA) overnight or with anti-mouse caspase-9 antibody (RD Systems) for 1 h. After the membrane had been washed in PBST, secondary antibody (anti-mouse HRP conjugated, RD Systems) in PBST was applied for 1 h. After washing, the protein bands were detected with the aid of the ECL enhanced chemiluminescence system (Amersham).

Cyclic voltammetry: Experiments were conducted with a computer-controlled Metrohm Eco Chemie Autolab PGSTAT 100 instrument with 1 mm diameter planar Pt and glassy carbon working electrodes, a Pt wire auxiliary electrode and an Ag wire reference electrode (isolated by a salt bridge containing 0.5 M Bu₄NPF₆ in CH₃CN). The reference electrode potential was calibrated in CH₂Cl₂ and CH₃CN with use of the ferrocene/ferrocenium redox couple as an external standard. HPLC-grade solvents were dried with molecular sieves (3 Å) under nitrogen prior to use and the test solution was deoxygenated by purging with argon.

Acknowledgements

We thank the Philipps-University Marburg, the Dr. Kleist-Stiftung Berlin, and the Natural Science Foundation of China (grant number 20925208) for financial support.

Keywords: antitumor agents · apoptosis · cytotoxicity · metallacycles · osmium

- [1] a) C. G. Hartinger, P. J. Dyson, *Chem. Soc. Rev.* **2009**, 38, 391–401; b) A. Levina, A. Mitra, P. A. Lay, *Metallomics* **2009**, 1, 458–470; c) T. W. Hambley, *Dalton Trans.* **2007**, 4929–4937; d) Y. K. Yan, M. Melchart, A. Habtemariam, P. J. Sadler, *Chem. Commun.* **2005**, 4764–4776.
- [2] H. Köpf, P. Köpf-Maier, *Angew. Chem.* **1979**, 91, 509–509; *Angew. Chem. Int. Ed. Engl.* **1979**, 18, 477–478.
- [3] P. M. Abeyasinghe, M. M. Harding, *Dalton Trans.* **2007**, 3474–3482.
- [4] K. Strohfeldt, M. Tacke, *Chem. Soc. Rev.* **2008**, 37, 1174–1187.
- [5] A. F. A. Peacock, P. J. Sadler, *Chem. Asian J.* **2008**, 3, 1890–1899.
- [6] P. J. Dyson, G. Sava, *Dalton Trans.* **2006**, 1929–1933.
- [7] S. Schäfer, I. Ott, R. Gust, W. S. Sheldrick, *Eur. J. Inorg. Chem.* **2007**, 3034–3046.
- [8] a) K. S. M. Smalley, R. Contractor, N. K. Haass, A. N. Kulp, G. E. Atilla-Gokcumen, D. S. Williams, H. Bregman, K. T. Flaherty, M. S. Soengas, E. Meggers, M. Herlyn, *Cancer Res.* **2007**, 67, 209–217; b) E. Meggers, G. E. Atilla-Gokcumen, K. Gründler, C. Frias, A. Prokop, *Dalton Trans.* **2009**, 10882–10888.
- [9] a) W. F. Schmid, R. O. John, V. B. Arion, M. A. Jakupec, B. K. Keppler, *Organometallics* **2007**, 26, 6643–6652; b) W. F. Schmid, R. O. John, G. Mühlgassner, P. Heffeter, M. A. Jakupec, M. Galanski, W. Berger, V. B. Arion, B. K. Keppler, *J. Med. Chem.* **2007**, 50, 6343–6355.
- [10] A. Vessières, S. Top, P. Pigeon, E. Hillard, L. Boubeker, D. Spera, G. Jaouen, *J. Med. Chem.* **2005**, 48, 3937–3940.
- [11] D. Schlawe, A. Majdalani, J. Velcicky, E. Heßler, T. Wieder, A. Prokop, H.-G. Schmalz, *Angew. Chem.* **2004**, 116, 1763–1766; *Angew. Chem. Int. Ed.* **2004**, 43, 1731–1734.
- [12] I. Ott, K. Schmidt, B. Kircher, P. Schumacher, T. Wiglenda, R. Gust, *J. Med. Chem.* **2005**, 48, 622–629.
- [13] Review on aromatic metallacycles: C. W. Landorf, M. M. Haley, *Angew. Chem.* **2006**, 118, 4018–4040; *Angew. Chem. Int. Ed.* **2006**, 45, 3914–3936.
- [14] H. Xia, G. He, H. Zhang, T. B. Wen, H. H. Y. Sung, I. D. Williams, G. Jia, *J. Am. Chem. Soc.* **2004**, 126, 6862–6863.
- [15] H. Zhang, L. Wu, R. Lin, Q. Zhao, G. He, F. Yang, T. B. Wen, H. Xia, *Chem. Eur. J.* **2009**, 15, 3546–3559.
- [16] Y. Lin, L. Gong, H. Xu, X. He, T. B. Wen, H. Xia, *Organometallics* **2009**, 28, 1524–1533.
- [17] L. Gong, Z. Chen, Y. Lin, X. He, T. B. Wen, X. Xu, H. Xia, *Chem. Eur. J.* **2009**, 15, 6258–6266.
- [18] L. Gong, Y. Lin, T. B. Wen, H. Xia, *Organometallics* **2009**, 28, 1101–1111.
- [19] P. R. Hoffman, K. G. Caulton, *J. Am. Chem. Soc.* **1975**, 97, 4221–4228.
- [20] L. Gong, Y. Lin, T. B. Wen, H. Zhang, B. Zeng, H. Xia, *Organometallics* **2008**, 27, 2584–2589.
- [21] It is also noteworthy that **OC10** has a reasonable solubility of approximately 0.75 mM in 10% DMSO/H₂O.
- [22] T. Decker, L.-M. Lohmann-Matthes, *J. Immunol. Methods* **1988**, 115, 61–69.
- [23] K.-M. Debatin, *Toxicol. Lett.* **2000**, 112–113, 41–48.
- [24] V. M. Rothenberg, V. Ling, *J. Natl. Cancer Inst.* **1989**, 81, 907–910.
- [25] R. Pieters, E. Klumper, G. J. L. Kaspers, A. J. P. Veerman, *Crit. Rev. Oncol. Hematol.* **1997**, 25, 11–26.
- [26] M. P. Murphy, *Biochim. Biophys. Acta, Bioenergetics* **2008**, 1777, 1028–1031.
- [27] J. L. Hickey, R. A. Ruhayel, P. J. Barnard, M. V. Baker, S. J. Berners-Price, A. Filipovska, *J. Am. Chem. Soc.* **2008**, 130, 12570–12571.
- [28] I. Nicoletti, G. Migliorati, M. G. Pagliacci, F. Grignani, C. Riccardi, *J. Immunol. Methods* **1991**, 139, 271–279.
- [29] C. Riccardi, I. Nicoletti, *Nat. Protocols* **2006**, 1, 1458–1461.
- [30] P. K. Smith, R. I. Krohn, G. T. Hermanson, A. K. Mallia, F. H. Gärtner, M. D. Provenzano, E. K. Fujimoto, N. M. Goeke, B. J. Olson, D. C. Klenk, *Anal. Biochem.* **1985**, 150, 76–85.

Received: January 31, 2010

Published online on June 23, 2010